*American Mineralogist, Volume 93, pages 996–1004, 2008*

# The crystal chemistry of Li in gadolinite

**FERNANDO CÁMARA,[1,*] ROBERTA OBERTI,[1] LUISA OTTOLINI,[1] GIANCARLO DELLA VENTURA,[1,2] AND FABIO BELLATRECCIA[2]**

[1]CNR-Istituto di Geoscienze e Georisorse, Unità di Pavia, Via Ferrata 1, I-27100 Pavia, Italy
[2]Dipartimento di Scienze Geologiche, Università degli Studi Roma Tre, I-00146 Roma, Italy

## ABSTRACT

This paper describes a multi-technique approach to the complete crystal-chemical characterization of a gadolinite-(Y) sample found in a volcanic holocrystalline ejectum near the Vico lake (Latium, Italy). Gadolinite-(Y) occurs as poly-twinned crystals forming rounded short-prismatic aggregates (generally 0.1–0.3 mm in size, with the largest ever found >1 mm), associated with zircon, thorite, danburite, betafite, and tourmaline.

Both the chemical and the structural characterization of gadolinite-(Y) from Vico required non-standard procedures. After correction for (100) twinning, the structure of a crystal with unit-cell dimensions $a$ = 4.7708(4) Å, $b$ = 7.6229(7) Å, $c$ = 9.8975(9) Å, β = 90.017(7)°, and $V$ = 359.95(6) Å$^3$ was refined in the $P2_1/c$ space group down to $R$ = 2.3%. Electron microprobe (EMP) analyses failed to give accurate quantification of major elements, due to the presence of light and volatile elements as well as of rare earth elements (REE) and actinides. Secondary ion-mass spectrometry (SIMS) analysis done with accurate calibrations on well-characterized minerals allowed quantification of light, volatile, REE, and actinide elements, and also of Ca and Si. The derived chemical composition was interpreted with reference to the site-scattering values obtained from single-crystal structure refinement. The resulting unit formula is $(Ca_{0.81}REE_{0.66}Y_{0.39}Th_{0.13}U_{0.02})_{\Sigma 2.01}(Fe^{2+}_{0.29}Li_{0.14}Fe^{3+}_{0.12}Mn_{0.02}Mg_{0.01})_{\Sigma 0.58}(Si_{1.98}Be_{1.09}B_{0.81}Li_{0.12})_{\Sigma 4.00}O_8(O_{1.20}F_{0.51}OH_{0.29})_{\Sigma 2.00}$, which yields a calculated density of 4.267 g cm$^{-3}$.

Fourier transform infrared spectroscopy (FTIR) single-crystal spectrum of gadolinite-(Y) shows several absorptions in the OH-stretching region that can be assigned to the different local configurations involving Ca and (REE,Y) at the A site and Be, B, and Li at the Z site.

Lithium incorporation in gadolinite-group minerals is proposed to occur according to the exchange vectors: (1) $^X Fe^{2+} + {}^A Y \rightarrow {}^X Li + {}^A(Th + U)$ and (2) $^Z Be + {}^X Fe^{2+} \rightarrow {}^Z Li + {}^X Fe^{3+}$; the maximum amount of Li allowed in the gadolinite structure is 1.0 apfu.

This work provides the first evidence that Li is a significant component in gadolinite-group minerals, particularly in geochemical environments enriched in actinides. This conclusion suggests that materials having the composition of Li-rich gadolinite may be considered as possible forms for radioactive waste disposal.

**Keywords:** Gadolinite, lithium, single crystal XRD, EMPA, SIMS, IR spectroscopy

## INTRODUCTION

Gadolinite-(Y), ideally $Y_2Be_2Fe^{2+}Si_2O_8O_2$ is a nesosilicate typically found in granite and alkaline granite pegmatite veins rich in alkaline-earth elements. Gadolinite group minerals (including hingganite and datolite) have the general formula $A_2Z_2X_xT_2O_8[O_{2x}(OH)_{2-2x}]$ where $0 \le x \le 1$, and $A$ = Y, REE, Ca; $Z$ = Be, B; $T$ = Si; and $X$ = either $Fe^{2+}$ or □. The hingganite series is generated from gadolinite by the exchange $Fe^{2+} + 2\ O^{2-} \rightarrow {}^X\square + 2\ OH^-$ yielding $Y_2Be_2Si_2O_8(OH)_2$, whereas the datolite series is generated from hingganite by the coupled exchange $(Y,REE^{3+}) + Be^{2+} \rightarrow Ca^{2+} + B^{3+}$ yielding $Ca_2B_2Si_2O_8(OH)_2$. Other related minerals isostructural with datolite are bakerite [$Ca_4B_5Si_3O_{15}(OH)_5$, Perchiazzi et al. 2004] and homilite [$Ca_2B_2FeSi_2O_8O_2$, Miyawaki et al. 1985].

Gadolinite-group minerals have a sheet-like structure composed of two different layers alternating along the [100] direction (when described in the $P2_1/c$ space group) and forming a stable 3-dimensional framework (Fig. 1a). One layer is made up by four- and eight-membered rings of tetrahedra (occupied by Si and Be in gadolinite and by Si and B in datolite, Fig. 1b). The other layer is made up by distorted tetragonal antiprisms containing large cations (Y or REE in gadolinite and hingganite, Ca in datolite) and distorted octahedra containing either $Fe^{2+}$ or 2 H atom bonded to the O5 atoms (Fig. 1c).

Gadolinite-group minerals are usually described in the $P2_1/a$ space group (Miyawaki et al. 1984, 1985; Anthony et al. 1995; Rastsvetaeva et al. 1996), whereas datolites are usually described in the $P2_1/c$ space group (Foit et al. 1973). To compare the relevant available data and to discuss the crystal chemistry of the solid-solution term under investigation, we have chosen to use in this paper the standard $P2_1/c$ setting.

Gadolinites are often metamict due to the presence of limited amounts of Th and U substituting for REE and/or Y (Segalstad

* E-mail: camara@crystal.unipv.it

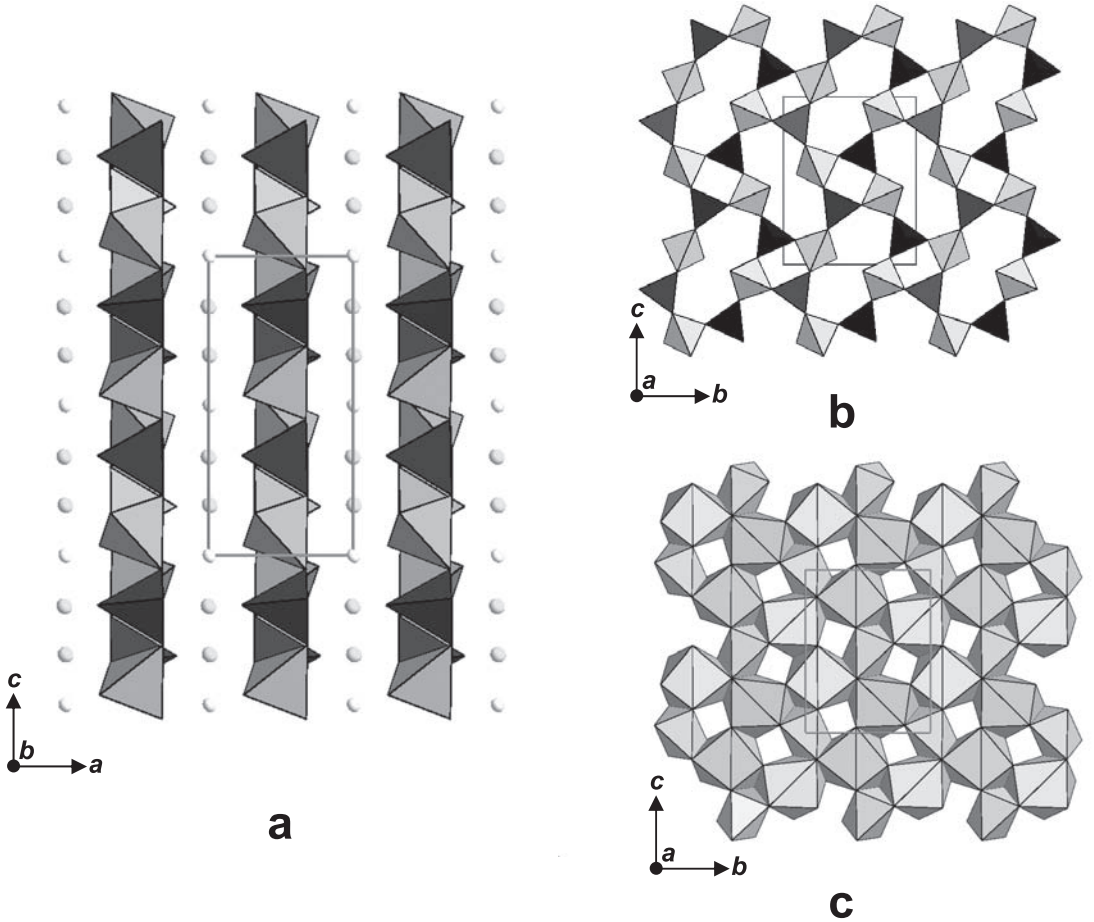


**FIGURE 1.** Crystal structure of gadolinite-(Y) (and of gadolinite-group minerals) in the space group $P2_1/c$. (**a**) The stacking of two different sheets alternating along the [100] direction. *Z* sites = dark gray, *T* sites = light gray, *A* sites = larger gray spheres, *X* sites = smaller light-gray spheres. (**b**) The (100) sheet made by corner-sharing $TO_4$ (light) and $ZO_4$ (dark) tetrahedral. (**c**) The (100) sheet of made by $AO_8$ polyhedra (dark) and $XO_6$ octahedra (light).

and Larsen 1978; Miyawaki et al. 1984), and hence good-quality crystallographic data are rare (Miyawaki et al. 1984; Demartin et al. 1993, 2001) or have been obtained on annealed samples (Segalstad and Larsen 1978). In addition, the presence of variable amounts of water and substitutions involving Be and B make microprobe analyses inadequate for their detailed crystal-chemical characterization. A further and presently unexplored feature of these minerals is the possible presence of significant Li in the structure, which can be however expected given the geochemical environment of formation.

Rastsvetaeva et al. (1996) and Pekov et al. (2000) examined a sample of "calcybeborosilite" from the unique locality of Dara-i-Pioz (Tajikistan), and noted similarities with the composition of gadolinite-(Y) from Vico first described by Della Ventura et al. (1990). "Calcybeborosilite" is isostructural with gadolinite, and represents an intermediate composition among hingganite-(Y) and datolite [although the authors claim it is a new valid species, it is still listed in the IMA-CNMNC report (version March 2007; http://www.geo.vu.nl/users/ima-cnmmn/MINERALlist.pdf) as published without approval of the CNMNC, and it is not included in Fleischer's Glossary of Mineral Species prepared by Mandarino and Back (2004)].

The mineral studied in this work had been reported as "mineral B" in holocrystalline ejecta of the Vico volcanic complex (Lazio, Italy) by Della Ventura et al. (1990). It is enriched in Th (and minor U), and particularly enriched in light-REE, an uncommon feature in gadolinite-group minerals. Due to its young age of formation (~150 k.y.: Sollevanti 1983; Laurenzi and Villa 1985), this sample is highly crystalline, thus allowing structure refinement of the unheated material.

We present in this paper the complete crystal-chemical characterization of this sample done combining secondary ion-mass spectrometry (SIMS), single-crystal X-ray diffraction (SREF), and infrared spectroscopy (FTIR). We also provide for the first time quantification of lithium in gadolinites, and discuss its crystal-chemical role in the gadolinite structure.

## GEOLOGICAL CONTEXT AND STUDIED SAMPLE

The occurrence of boron-rich minerals in the Roman Comagmatic Province is well known , and is related to the very high B content (up to 10× the value typical of basaltic rocks, i.e., 5–10 ppm, Vaselli and Conticelli 1990) of the volcanic rocks emitted

during the plio-pleistocenic volcanic activity of central Italy. Most of this unusual mineralogy is indeed observed within the tephra scattered at random in the pyroclastic deposits (e.g., Della Ventura et al. 1999) outcropping from south Tuscany down to Campania. Scherillo (1940) described danburite $CaB_2Si_2O_8$ and tourmaline $Na(Li,Al)_3Al_6(BO_3)_3[Si_6O_{18}](OH)_3(OH)$ in the holocrystalline ejecta from the Vico and Cimino volcanic complexes, Latium. Minerals of the vonsenite-ludwigite group, $(Fe^{2+},Mg)_2Fe^{3+}BO_5$, are known to be widespread in volcanic xenoliths and in pyroclastic rocks especially in the Alban Hills, Sabatini and Vico volcanic complexes (Federico 1957; Burragato 1963; Bachechi et al. 1966). Since then, and particularly in the last ten years, several rare or new B-bearing minerals have been described; the long list of these include, among the others, peprossiite-(Ce) (Della Ventura et al. 1993; Callegari et al. 2000), stillwellite-(Ce) (Burns et al. 1993), vicanite-(Ce) (Maras et al. 1995), and several minerals of the hellandite group, such as hellandite-(Ce) (Oberti et al. 1999), mottanaite-(Ce), ciprianiite (Della Ventura et al. 2002), and piergorite-(Ce) (Boiocchi et al. 2006).

The studied gadolinite-(Y) occurs as very small (generally up to 300 μm in maximum dimension) light-blue crystals within a 25 × 25 × 10 cm sized syenitic ejectum laying on the ground some 150 m away from the southeast shore of the Vico Lake, with no clear relationship to any ignimbritic horizon (Locardi 1965) of the Vico volcanic complex. The ejectum was discovered by Salvatore Fiori, who supplied samples for mineralogical characterization. The host rock is massive, darkish, fine grained, and contains rare sanidine phenocrystals up to 1 cm in size, and few mica aggregates. The clefts in-between the sanidine crystals are coated by small crystals of zircon, thorite, danburite, betafite, and tourmaline, along with the blue mineral, which occurs as polytwinned crystals forming rounded short-prismatic aggregates (0.1–0.3 mm in size, with the largest ever found >1 mm).

## Methods and techniques

### Electron microprobe

Chemical analyses of Fe, Mn, Mg, and Al were performed with a JEOL-JXA 8600 electron microprobe at CNR-IGG Firenze under the following conditions: 2–3 μm beam diameter, 15 kV excitation voltage, 15 nA beam current. Element concentrations were measured using the *K*α line in wavelength-dispersive spectrometry (WDS), and the following standards and analytical crystals were used: olivine (Mg, TAP), spessartine (Al, TAP and Mn, LIF), and ilmenite (Fe, LIF). Data reduction was done using a standard ZAF procedure. Due to the large number of unanalyzed elements (particularly light elements H, B, Be, and F), the values obtained by routinely acquired electron-probe analyses suffer from important matrix effects and did not fit with the results of the structure refinement. Therefore, a feedback procedure has been performed using the elemental quantification obtained by SIMS (cf. the next paragraph) to correct for various matrix effects affecting the electron microprobe analysis (for instance, emitted X-ray absorbance in the sample) and allow quantification of the EMP-analyzed elements. This procedure was re-cycled until convergence and gave the results reported in Table 1.

### Secondary ion mass spectrometry (SIMS)

Secondary ion mass spectrometry (SIMS) is generally employed to measure the concentrations of trace elements by means of an empirical approach to quantification. Matrix effects, i.e., non-linear effects relating ion intensities to elemental concentrations, increase considerably with increasing elemental contents. Hence, SIMS is rarely employed in major-element analysis. In the present study, we extended the capability of the SIMS technique to quantify a wide range of constituents, including major cations such as Si and Ca, to overcome the problems encountered during EMP analysis. Based on the similarity of the chemical composition, a well-characterized sample of Th-rich hellandite from Capranica (Oberti et al. 1999; Ottolini and Oberti 2000) was used as the SIMS primary standard for Si and Ca. SIMS matrix effects were thus calibrated by comparing the $^{30}Si^+$ and $^{44}Ca^+$ ion signals in the gadolinite sample with those monitored in hellandite. The absolute quantitative analysis of Si and Ca was achieved by a strict control of both instrumental parameters (among all, the primary ion-beam current intensity and focusing conditions) and the experimental ones, in particular, the waiting times (before SIMS analysis) and the acquisition (i.e., analytical) ones. Secondary positive ions were detected at the following masses (in amu): 30 (Si), 44 (Ca), 89 (Y), 137 (Ba), 139 (La), 140 (Ce), 141 (Pr), 146 (Nd), 149 (Sm), 163 (Dy), 167 (Er), 174 (Yb), 232 (Th), and 238 (U). $^{208}Pb^+$ was also monitored and quantified. Signals of Eu and Gd ion were obtained by deconvolution of the secondary-ion mass spectrum at mass numbers 151, 154, 160, and 162. The analysis of 1 (H), 7 (Li), 9 (Be), 11 (B), and 19 (F) was done on a different day to allow the crystal to degas under a vacuum of ~$10^{-7}$ Pa with the proper H-reference samples in the dual specimen-holder inlet-chamber. $^{30}Si^+$ was used as the internal reference for the matrix for Li, Be, B, U, Th, and Pb, whereas both $^{44}Ca^+$ and $^{30}Si^+$ were used for the quantification of H and F. Analysis was done after 10 min bombardment at the same points previously investigated for REE and other trace elements. To avoid any topographic effect due to the pre-existing craters, the crystal was polished smooth before analysis and then gold coated. The list of all the calibration standards employed (fully described in Oberti et al. 1999; Ottolini and Oberti 2000; Ottolini et al. 2002) was the following: Snarum apatite, NIST SRM 610, LL Std b, hellandite-(Ce) from Capranica, Pyrex glass, topaz crystal, Ceran glass. The estimated accuracy is in the range 5–15% rel. for

**Table 1.** Chemical analysis and chemical formula calculated on the basis of 10 (O + F) atoms per formula unit (apfu) for gadolinite -(Y) from Vico

| | Vico | Dara-i-Pioz | | Vico | Dara-i-Pioz | | Vico | Dara-i-Pioz | | Vico | Dara-i-Pioz |
|---|---|---|---|---|---|---|---|---|---|---|---|
| $SiO_2$ | 25.58 | 28.78 | $Dy_2O_3$ | 1.44 | 0.94 | Si | 1.977 | 2.004 | Nd | 0.169 | 0.027 |
| $Al_2O_3$ | 0.08 | | $Ho_2O_3$ | | 0.22 | B | 0.807 | 1.179 | Sm | 0.041 | 0.004 |
| FeO | 4.50 | 4.02* | $Er_2O_3$ | 0.81 | 1.25 | Be | 1.086 | 0.622 | Eu | 0.003 | |
| $Fe_2O_3$ | 2.14 | | $Tm_2O_3$ | | 0.23 | Li | 0.123 | | Gd | 0.033 | 0.008 |
| MnO | 0.31 | 0.80 | $Yb_2O_3$ | 0.98 | 1.59 | Al | 0.007 | | Tb | | 0.001 |
| MgO | 0.12 | | $Lu_2O_3$ | | 0.17 | Σ *T* + *Z* | 4.000 | 3.805 | Dy | 0.036 | 0.021 |
| CaO | 9.80 | 12.91 | $ThO_2$ | 7.49 | 0.62 | | | | Ho | | 0.005 |
| BeO | 5.85 | 3.72 | $UO_2$ | 1.42 | 2.29 | $Fe^{2+}$ | 0.291 | 0.234 | Er | 0.020 | 0.027 |
| $B_2O_3$ | 6.05 | 9.81 | F | 2.08 | 0.57 | $Fe^{3+}$ | 0.124 | | Tm | | 0.005 |
| $Li_2O$ | 0.83 | | $H_2O$ | 0.56 | 2.91† | Li | 0.135 | | Yb | 0.023 | 0.034 |
| $Y_2O_3$ | 9.39 | 19.82 | | 100.50 | 98.06 | $Mn^{2+}$ | 0.020 | 0.047 | Lu | | 0.004 |
| $La_2O_3$ | 2.04 | 1.51 | O=F | 0.87 | 0.24 | Mg | 0.014 | | Th | 0.132 | 0.010 |
| $Ce_2O_3$ | 8.49 | 3.92 | Total | 99.63 | 97.82 | Σ *X* | 0.584 | 0.281 | U | 0.024 | 0.035 |
| $Pr_2O_3$ | 1.46 | 0.34 | | | | | | | Σ *A* | 2.017 | 2.026 |
| $Nd_2O_3$ | 6.12 | 1.08 | | | | Ca | 0.811 | 0.963 | | | |
| $Sm_2O_3$ | 1.55 | 0.17 | REE | 0.664 | 0.284 | Y | 0.386 | 0.734 | O | 1.203 | 0.522 |
| $Eu_2O_3$ | 0.13 | | REE/Y | 1.720 | 0.387 | La | 0.058 | 0.039 | F | 0.508 | 0.126 |
| $Gd_2O_3$ | 1.28 | 0.34 | Ca/Y | 2.101 | 1.312 | Ce | 0.240 | 0.100 | OH | 0.289 | 1.353 |
| $Tb_2O_3$ | | 0.05 | Be/(B+Be) | 0.574 | 0.345 | Pr | 0.041 | 0.009 | Σ | 2.000 | 2.000 |

*Notes:* The chemical analysis and chemical formula of the "calcybeborosilite-(Y)" from Dara-i-Pioz, Tajikistan (Pekov et al. 2000) are shown for comparison.
* Total Fe as FeO.
† Calculated on the basis of stoichiometry by assuming OH + $O^{2-}$ + F = 2 apfu.

all the elements. An average of SIMS analyses over three data points is shown in Table 1, and is compared with the available chemical information for the sample from Dara-i-Pioz (Rastsvetaeva et al. 1996; Pekov et al. 2000). Unit formulae were calculated based on 10 (O + F) atoms per formula unit (apfu).

### Single-crystal X-ray diffraction (SREF)

Several crystals of gadolinite-(Y) were mounted on a Philips PW-1100 diffractometer, and examined with graphite-monochromatized Mo$K\alpha$ X-radiation; crystal quality was assessed via profile analysis of Bragg diffraction peaks. Although the β angle is close to 90°, evidences were found of peak splitting related to (100) twinning. A crystal 0.16 × 0.16 × 0.08 mm in size was used for data collection of two monoclinic *hkl* and $h\bar{k}l$ equivalents in the θ range 2–30°. Reflection profiles were integrated following the method of Lehmann and Larsen (1974) as modified by Blessing et al. (1974). Intensities were corrected for Lorentz-polarization and absorption following North et al. (1968), and then averaged and reduced to structure factors (*F*). Unit-cell dimensions were calculated from least-squares refinement of the *d* values obtained from 50 rows of the reciprocal lattice by measuring the gravity centroid of each reflection and its corresponding antireflection in the θ range –30° to 30°.

A weighted full-matrix least-squares refinement on $F^2$ was done using SHELXTL (Sheldrick 1997). Scattering curves for fully ionized chemical species were used at those sites where chemical substitutions occur ($Be^{2+}$ and B at the *Z* site, fully ionized curve is not available for boron; $Fe^{2+}$ at the *X* site; and $Ca^{2+}$ and $Th^{4+}$ at the *A* site); neutral vs. ionized scattering curves were used at the *T* and anion sites (except O5, where the curves for $O^{2-}$ and $F^-$ were used). The refinement of the structure was started with the coordinates of gadolinite-(Y) given by Miyawaki et al. (1984) transformed in space group $P2_1/c$, and yielded high *R*-factors and the presence of intense spurious maxima in the Fourier-difference maps. Therefore, a (100) twin matrix was applied, and the relative percentage of the twins was refined (to 0.57:0.43). The observed *R*-factor dropped to 2.3%. Selected crystal data and refinement information for the sample studied in this work are given in Table 2. Residual maxima in the Fourier-difference maps calculated at convergence were related to static disorder at the *A* site, where many species with different ionic radii occur. This feature and the low amount of H (as obtained by SIMS quantification), did not allow location of the H atoms of the OH groups in the Fourier-difference maps. Atom coordinates and isotropic displacement parameters are reported in Table 3. Errors in the x/*a* coordinates of all atoms are higher than for the other fractional coordinates due to the presence of (100) twinning (Table 3). Observed and calculated structure factors are reported in Table 4[1]. Selected interatomic distances are reported in Table 5.

**TABLE 2.** Selected crystal data and refinement information for gadolinite-(Y) from Vico

| | Vico | Dara-i-Pioz |
|---|---|---|
| *a* (Å) | 4.771(1) | 4.766(2) |
| *b* (Å) | 7.623(1) | 7.600(2) |
| *c* (Å) | 9.898(1) | 9.846(4) |
| β (°) | 90.02(1) | 90.11(3) |
| *V* (Å$^3$) | 360.0(1) | 356.6(2) |
| no. $F_{all}$ | 1053 | 1575 |
| no. $F_{obs}$ ($F > 3\sigma_F$) | | 775 |
| $R_{sym}$ | 2.02 | 2.80 |
| $R_{obs}$ ($F > 3\sigma_F$) | | 6.20 |
| $R_{all}$ | 2.34 | n.r. |
| size (mm) | 0.16 × 0.16 × 0.08 | 0.35 × 0.30 × 0.25 |
| θ-range | 2–30° | 0–31.7° |

*Notes:* Crystal data for the "calcybeborosilite-(Y)" from Rastsvetaeva et al. (1996) are also shown for comparison. n.r. = not reported.

### Infrared spectroscopy

Single-crystal micro-FTIR spectra were collected with a NicPlan microscope, equipped with a MCT-A nitrogen-cooled detector and a KBr beamsplitter. Nominal resolution was 4 cm$^{-1}$ and final spectra are the average of 128 scans. The unpolarized-light spectrum of gadolinite-(Y) from Vico is compared in Figure 2 with the spectrum of datolite from Pitigliano, recently described by Bellatreccia et al. (2006). The OH-stretching spectrum of datolite shows a unique sharp band at 3497 cm$^{-1}$, whereas that of gadolinite consists of a broad absorption that can be resolved by two overlapping main components at 3552 and 3523 cm$^{-1}$, and two shoulders at 3600 and 3475 cm$^{-1}$.

## THE CRYSTAL-CHEMICAL FORMULA OF GADOLINITE-(Y) FROM VICO

The results of the structure refinement (in terms of site-scattering values and mean bond distances) were used to check for the

[1] Deposit item AM-08-034, Table 4 (observed and calculated structure factors) and CIF. Deposit items are available two ways: For a paper copy contact the Business Office of the Mineralogical Society of America (see inside front cover of recent issue) for price information. For an electronic copy visit the MSA web site at http://www.minsocam.org, go to the American Mineralogist Contents, find the table of contents for the specific volume/issue wanted, and then click on the deposit link there.

**TABLE 3.** Atom coordinates, site-scattering values, equivalent isotropic and anisotropic displacement parameters (Å$^2$) for gadolinite-(Y) from Vico

| Atom | s.s.* | x/a | y/b | z/c | $U_{eq}$ | $U_{11}$ | $U_{22}$ | $U_{33}$ | $U_{23}$ | $U_{13}$ | $U_{12}$ |
|---|---|---|---|---|---|---|---|---|---|---|---|
| O1 | 8.00 | 0.2408 (5) | 0.4052 (3) | 0.0343 (2) | 0.010 (1) | 0.008 (1) | 0.013 (1) | 0.010 (1) | 0.001 (1) | 0.000 (1) | 0.001 (1) |
| O2 | 8.00 | 0.6723 (5) | 0.2924 (3) | 0.4542 (2) | 0.011 (1) | 0.013 (1) | 0.009 (1) | 0.012 (1) | 0.001 (1) | 0.005 (1) | 0.000 (1) |
| O3 | 8.00 | 0.6834 (5) | 0.3401 (3) | 0.2024 (2) | 0.012 (1) | 0.013 (1) | 0.013 (1) | 0.010 (1) | 0.000 (1) | –0.002 (1) | –0.003 (1) |
| O4 | 8.00 | 0.3173 (5) | 0.0968 (3) | 0.1432 (2) | 0.011 (1) | 0.015 (1) | 0.009 (1) | 0.008 (1) | 0.001 (1) | 0.003 (1) | –0.005 (1) |
| O5 | 8.14 (6) | 0.2270 (4) | 0.4105 (3) | 0.3350 (3) | 0.011 (1) | 0.010 (1) | 0.013 (1) | 0.010 (1) | 0.000 (1) | 0.000 (1) | 0.001 (1) |
| *T* | 14.00 | 0.4765 (2) | 0.2704 (1) | 0.0813 (1) | 0.006 (1) | 0.007 (1) | 0.006 (1) | 0.006 (1) | 0.000 (1) | 0.000 (1) | –0.001 (1) |
| *Z* | 4.27 (4) | 0.5462 (6) | 0.4106 (4) | 0.3384 (4) | 0.006 (1) | 0.005 (2) | 0.006 (1) | 0.006 (1) | 0.000 (1) | –0.001 (2) | –0.001 (1) |
| *X* | 12.24 (0) | 0 | 0 | 0 | 0.007 (1) | 0.006 (1) | 0.008 (1) | 0.007 (1) | 0.001 (1) | –0.001 (1) | 0.001 (1) |
| *A* | 41.7 (2) | 0.9958 (1) | 0.1068 (1) | 0.3309 (1) | 0.009 (1) | 0.008 (1) | 0.009 (1) | 0.008 (1) | 0.000 (1) | –0.001 (1) | 0.001 (1) |

*Note:* $U_{eq}$ is defined as one third of the trace of the orthogonalized $U_{ij}$ tensor; the anisotropic displacement parameter has the form: $-2\pi^2[h^2a^{*2}U^{11} + ... + 2hka^*b^*U^{12}]$.

* Site-scattering values (electrons per site).

**TABLE 5.** Selected bond lengths (Å) for gadolinite-(Y) from Vico and for the "calcybeborosilite-(Y)" from Rastsvetaeva et al. (1996)

| | Vico | Dara-i-Pioz | | Vico | Dara-i-Pioz |
|---|---|---|---|---|---|
| T-O1 | 1.593(2) | 1.603(9) | Z-O2 | 1.578(4) | 1.560(9) |
| T-O2 | 1.638(2) | 1.629(9) | Z-O3 | 1.591(4) | 1.600(9) |
| T-O3 | 1.641(2) | 1.613(9) | Z-O4 | 1.572(4) | 1.580(9) |
| T-O4 | 1.644(3) | 1.670(9) | Z-O5 | 1.523(4) | 1.480(9) |
| <T-O> | 1.629 | 1.629 | <Z-O> | 1.566 | 1.555 |
| X-O2 x2 | 2.270(2) | 2.257(8) | A-O1 | 2.327(2) | 2.308(8) |
| X-O4 x2 | 2.201(2) | 2.170(9) | A-O1 | 2.329(2) | 2.332(8) |
| X-O5 x2 | 2.075(3) | 2.113(8) | A-O2 | 2.424(2) | 2.413(9) |
| <X-O> | 2.182 | 2.180 | A-O3 | 2.646(2) | 2.570(9) |
| | | | A-O3 | 2.566(2) | 2.630(9) |
| | | | A-O4 | 2.411(2) | 2.350(9) |
| | | | A-O5 | 2.565(2) | 2.570(8) |
| | | | A-O5 | 2.463(2) | 2.448(8) |
| | | | <A-O> | 2.466 | 2.453 |

analytical data and to distribute the elements over the structural sites. Some further comments are however required to explain the criteria used to calculate the unit formulae in Table 1.

First of all, because there is a deficit of usual fourfold-coordinated cations in gadolinite-group minerals, the analyzed Li content was distributed over the Z and the X sites. Noteworthy, both Si + Al and B + Be + Li sum to 2 apfu, showing a different site preference of the fourfold-coordinated cations. In the gadolinite group, the size of the *Z* tetrahedron is evaluated excluding the *Z*-O5 distance, which is affected by OH-F-$O^{=}$ substitution ($^{-O5}$<Z-O>; see Demartin et al. 1993 and 2001 for a discussion). $^{-O5}$<Z-O> for the sample of this work is 1.579 Å, i.e., the value

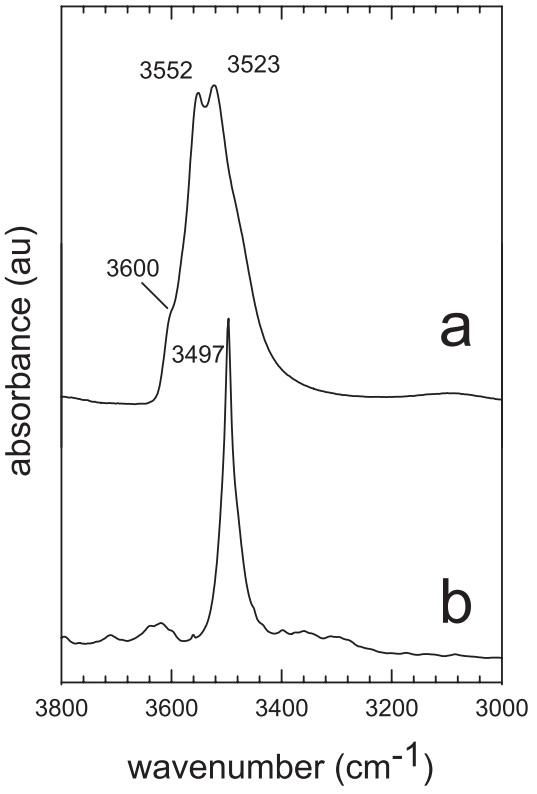


**FIGURE 2.** Single-crystal FTIR spectrum of (**a**) gadolinite-(Y) from Vico and (**b**) datolite from Pitigliano (Tuscany), sample from Bellatreccia et al. (2006).

expected considering the ionic radii reported by Shannon (1976), namely Li = 0.59, Be = 0.27, and B = 0.11 Å. The substitution of Li after Be in the tetrahedron, although uncommon, has been already observed and well documented in the hellandite group minerals (Oberti et al. 2002). Hellandite samples coming from the same locality of the studied gadolinite show contents of tetrahedral Li up to 0.24 apfu. Li also substitutes Be in the tetrahedron in Cs-rich beryl pezzottaite [$Cs(Be_2Li)Al_2Si_6O_{18}$, Hawthorne et al. 2004].

Demartin et al. (2001) gave a predictive plot to calculate the Be/(Be + B) ratio in gadolinite from the $^{-O5}$<Z-O> distance. For the sample of this work, we obtain a Be/(Be + B) ratio around 0.60, slightly higher than the experimental value (0.57; Table 1). The difference is probably due to the effect of the 5% occupancy of Li at the *Z* site, which could not be taken into account by Demartin et al. (2001).

Previous work on natural and synthetic gadolinites suggested the presence of $Fe^{3+}$ (Nakai 1938; Ito 1967), which was confirmed by Mössbauer spectroscopy in synthetic calciogadolinite, $CaYBe_2Fe^{3+}Si_2O_8O_2$ (Ito and Hafner 1974). In contrast, Demartin et al. (1993) did a systematic investigation of gadolinite-group minerals from the Alps and proposed, on the basis of the observed <*X*-O> distances, that iron is all in the divalent state in these samples. The sample under investigation has a large <*X*-O> distance; however, the incorporation of Li in the *Z* tetrahedron implies that part of the iron is in the trivalent state (see below).

The crystal-chemical formula proposed in Table 1 is $^{A}(Ca_{0.81}REE_{0.66}Y_{0.39}Th_{0.13}U_{0.02})_{\Sigma 2.01}$ $^{X}(Fe^{2+}_{0.29}Li_{0.14}$ $Fe^{3+}_{0.12}Mn_{0.02}Mg_{0.01})_{\Sigma 0.58}$ $^{Z,T}(Si_{1.98}Be_{1.09}B_{0.81}Li_{0.12})_{\Sigma 4.00}$ $O_8(O_{1.20}F_{0.51}OH_{0.29})_{\Sigma 2.00}$. In this formula, (REE+Y) > Ca, and Y is predominant over REE; also Be > B, and the sum of the cations at the X site > 0.5. Therefore, the sample from Vico is classified as gadolinite-(Y). Noteworthy, the B, Ca, and (F+OH) contents are nearly equal (with F dominant over OH), thus the sample under investigation has a composition close to a 60:40 term along the ideal gadolinite-"fluoro-datolite" solid-solution. Note also that the incorporation of (F,OH) at the O5 site involves an equal amount of vacancy at the *X* site. The SIMS data reported in Table 1 are averaged over three point analyses, and e.s.d. values (1σ) are consistent with sample inhomogeneity. For example, the scatter by ~ 30% (as 1σ%) in the average $Nd_2O_3$ concentration (6.12 wt%) is much higher than the analytical uncertainty of the SIMS quantification procedure. The same observation holds for $Gd_2O_3$ [1.28 ± 0.36(1σ) (wt%)], $Sm_2O_3$ [1.55 ± 0.57(1σ) (wt%)], and $UO_2$ [1.42 ± 0.73(1σ) (wt%)].

The refined and calculated site-scattering values (in electrons per formula unit, epfu) are in excellent agreement, the overall discrepancy being within 2% rel., well within the overall uncertainty of the analysis. Focusing on the various sites, we find 8.54 vs. 8.75 epfu at the *Z* site, and 12.24 vs. 11.98 epfu at the *X* site. Interestingly, the mean <*X*-O> distance (2.182 Å) is close to the value given for "calcybeborosilite-(Y)" (2.180 Å), notwithstanding the halved *X*-site occupancy of the latter. There are two possible explanations for this evidence: (1) some undetected Li could be present in the sample from Dara-i-Pioz, the *X*-site occupancy thus being underestimated; (2) the dimension of the *X* site in gadolinite-group minerals is rather invariant (in agreement with the available structural data, where <*X*-O>

varies only from 2.152 to 2.200 Å).

The refined site-scattering at the *A* site is 83.35 epfu, slightly lower than the calculated value (85.34 epfu). This discrepancy may be related to the presence at this site of cations with different ionic radii. Residual peaks observed in the difference Fourier map confirm that the electron density has not been fully taken into account in the refined model, and that the refined site-scattering value may be slightly underestimated.

The chondrite-normalized REE pattern calculated from SIMS analysis (Fig. 3) is enriched in REE (but depleted in La); the overall shape of the pattern is similar to the one given by Oberti et al. (1999) for a Th-rich hellandite-(Ce) from the same volcanic deposit. In gadolinite-(Y), however, REE are less fractionated than in hellandite-(Ce), $(Ce/Yb)_{ch}$ being 2.18 and 18.9, respectively. Both minerals are characterized by a negative Eu anomaly, which can be related to the presence of sanidine in the paragenesis: the values for Eu/Eu* result to be 0.285 in gadolinite-(Y) and 0.371 in hellandite-(Ce).

## Exchange vectors ruling Li incorporation in the gadolinite structure

The unit formula reported in Table 1 can be used to discuss some crystal-chemical features of the studied sample and to model the mechanisms ruling the incorporation of Li in gadolinite-group minerals. The sample from Vico can be related to gadolinite-(Y) by several heterovalent substitutions. We have already noted above that the amounts of B, Ca and (F+OH, with F > OH) contents are equal (0.81 apfu), thus suggesting that this sample is the 60:40 term in the gadolinite-"fluoro-datolite" solid solution. Based on structure topology (Fig. 4) and the observed chemical variations, there are five exchange vectors involving Li that allow satisfaction of bond-strength requirements at the relevant O atoms: (1) $^{X}Fe^{2+} + {}^{A}Y \rightarrow {}^{X}Li + {}^{A}(Th + U)$; (2) $^{Z}Be + {}^{A}Y \rightarrow {}^{Z}Li + {}^{A}(Th + U)$; (3) $^{Z}Be + {}^{X}Fe^{2+} \rightarrow {}^{Z}Li + {}^{X}Fe^{3+}$; (4) $^{Z}Be + {}^{X}\square \rightarrow {}^{Z}Li + {}^{X}Li$, which would also imply either the simultaneous exchange $OH \rightarrow O^{2-}$ or the presence of F at the O5 site; and (5) $2\ {}^{X}Fe^{2+} \rightarrow {}^{X}Li + {}^{X}Fe^{3+}$. The exchange vector 4 would explain the nearly equal Li contents observed at the *X* and *Z* sites. However, vector 4 would not account for the (Th + U) content and for the fact that the sum of the *X*-site occupancy and (OH + F)/2 is close to 1 apfu. It is thus discarded, at least for the sample under investigation.

We are thus left with two possibilities for Li incorporation at the *X* site, i.e., the exchange vectors 1 and 5, which implies incorporation of (Th + U) at the *A* site and of $Fe^{3+}$ at the *X* site, respectively. Given the total amount of $^{A}(Th + U)$ in the sample under investigation, the exchange vector 2 can also be discarded. Hence, incorporation of Li at the *Z* site must be related to the (partial) oxidation of Fe occurring at the *X* site. This is the reason why the unit formula of gadolinite-(Y) was recalculated in Table 1 to allow for a $^{X}Fe^{3+}$ content equal to the (Be + B) deficiency at the *Z* site, i.e., to the amount of $^{Z}Li$. The exchange vector 5 may however account for oxidation of $Fe^{2+}$ to $Fe^{3+}$, but does not explain the observed cation deficiency at the Z site.

The maximum amount of Li which can be incorporated into the gadolinite structure is limited by the stoichiometry of the end-members and the relations between the exchange vectors 1, 3, and 5. Mechanism 1 would produce lithium dominance at the *X* site, and thus an hypothetical end-member "thorium-lithium gadolinite," $^{A}(ThY)^{Z}Be_2{}^{X}Li^{T}Si_2O_8O_2$. In contrast, mechanism 3 cannot produce lithium dominance, and is limited to the $^{A}Y_2{}^{Z}(BeLi)^{X}Fe^{3+T}Si_2O_8O_2$ component. Also mechanism 5 cannot produce lithium dominance at the *X* site, the limit being 0.5 Li apfu. When the exchange vectors 1, 3, and 5 act simultaneously, the $^{X}Li$ content from mechanism 1 is incompatible with the $^{X}Fe^{3+}$ content from mechanisms 3 and 5, and thus the maximum amount of Li allowed is always limited to 1.0 apfu.

## Geometrical changes due to the incorporation of Li in the gadolinite structure

Due to the similarity of the ionic radii (Li = 0.76, $Fe^{2+}$ = 0.78 Å; Shannon 1976), incorporation of lithium into the *X* octahedron is not expected to decrease significantly its size. A similar but complementary change in volume is however obtained at the *A* site by the substitution of Th (1.05 Å) after Y (1.02 Å). Thus mechanism 1 is not expected to change significantly the unit-cell dimensions and volume.

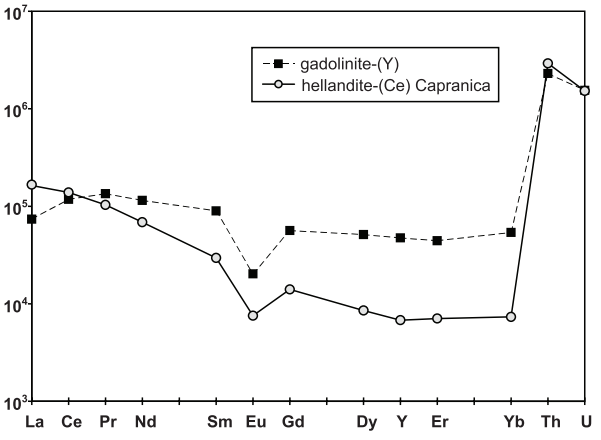


**FIGURE 3.** Chondrite-normalized trace element pattern of gadolinite-(Y) from Vico and hellandite-(Ce) from Capranica [normalization factors C1 from Anders and Ebihara (1982)].

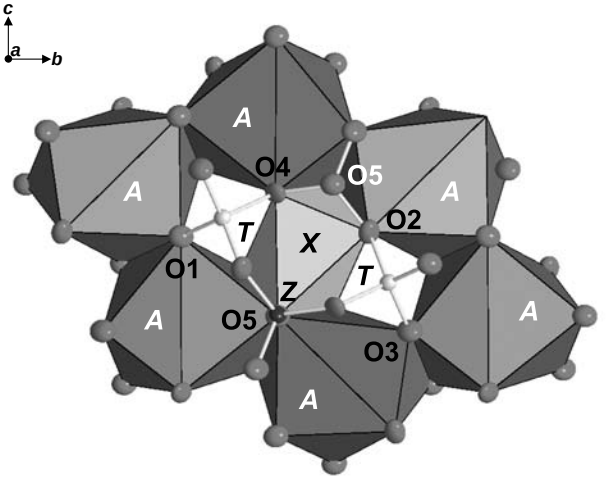


**FIGURE 4.** Detail of the crystal structure of gadolinite-(Y) (and of gadolinite-group minerals) in the space group $P2_1/c$ showing the local environment around the *X* site.

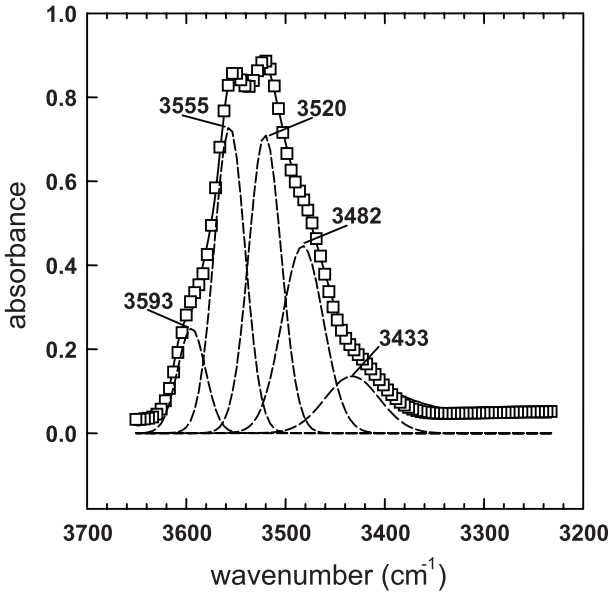


**FIGURE 5.** The spectrum of gadolinite-(Y) from Vico resolved into Gaussian components. For explanation, see text.

In contrast, mechanism 3 must produce a significant enlargement of the *Z* tetrahedron (Li = 0.59 Å, Be = 0.27 Å), which is coupled with a far smaller shrinkage of the *X* octahedron ($Fe^{2+}$ = 0.78 Å, $Fe^{3+}$ = 0.645 Å). Given that the composition of the *T* tetrahedron is almost fixed to pure Si in gadolinite-group minerals, the increase in size of the *Z* tetrahedron should not provoke a strong increase in the *a* edge, but rather a wrinkling of the sheet of tetrahedra.

Mechanism 5 should produce a shrinkage of the *X* octahedron as both Li and $Fe^{3+}$ are smaller than $Fe^{2+}$. Because it is not accompanied by a change in the size of the adjacent polyhedra, it would promote deformation of the adjacent *A* sites. In contrast, the available structural data show that the mean <*X*-O> bond distance is rather independent from *X*-site occupancy.

## SHORT-RANGE ORDER DUE TO LI INCORPORATION IN GADOLINITE

All the evidences discussed above imply a strong short-range order in the gadolinite structure, in particular concerning the cations closest to the *X* sites (cf. Fig. 4). In the sample of this work, both the F atoms and the OH groups at the O5 site must be associated with one Ca atom and one (Y, REE) atom at the adjacent *A* sites, and with two B atoms at the adjacent *Z* sites. This situation is somewhat intermediate between datolite (with two $^{A}$Ca atoms and two $^{Z}$B atoms) and hingganite (with two $^{A}$Y atoms and two $^{Z}$Be atoms).

In contrast, the Li atoms at the *X* site should be associated with one ($Th^{4+}$, U), three (Y, REE) atoms at the adjacent *A* sites, and four Be atoms at the *Z* sites, whereas the $Fe^{3+}$ atoms at the *X* site must be associated with four $^{A}$(Y, REE) atoms, one $^{Z}$Li and three $^{Z}$Be atoms.

The occurrence of $Fe^{3+}$ at the *X* site should also provoke a local order of the larger LREE in the surrounding *A* site, which would help to maintain a regularity in the dimensions of the sheet. Actually, the anomalous enrichment in LREE in gadolinite-(Y) from Vico fits well with the anomalous presence of $^{X}Fe^{3+}$ (at least, compared to Alpine gadolinites) and of $^{Z}$Li.

When considering the formal bond-valence incident to the O2 and O4 atoms, we obtain the following situations and valence units (v.u.): (1) (OH, F) at O5: both O2 and O4 coordinate $^{VIII}Ca^{2+}$ + $^{IV}Si^{4+}$ + $^{IV}B^{3+}$, and their formal bond-valence is 0.25 + 1.00 + 0.75 = 2.00 v.u.; (2) Li at the *X* site: both O2 and O4 coordinate $^{VIII}(Th^{4+}, Y^{3+})$ + $^{IV}Si^{4+}$ + $^{IV}Be^{2+}$ + $^{VI}Li^{+}$, and the formal bond-valence is 0.438 + 1.00 + 0.50 + 0.166 = 2.104 v.u.; (3) $Fe^{3+}$ at the *X* site: both O2 and O4 coordinate $^{VIII}Y^{3+}$ + $^{IV}Si^{4+}$ + $^{IV}Li^{+}$ + $^{VI}Fe^{3+}$, and the formal bond-valence is 0.375 + 1.00 + 0.25 + 0.50 = 2.125 v.u.; and (4) $Fe^{2+}$ at the *X* site: both O2 and O4 coordinate $^{VIII}Y^{3+}$ + $^{IV}Si^{4+}$ + $^{IV}Be^{2+}$ + $^{VI}Fe^{2+}$, and the formal bond-valence is 0.375 + 1.00 + 0.50 + 0.333 = 2.208 v.u.

The slight excess of bond valence incident to the O2 and O4 O atoms in the presence of an *X* cation can be compensated by relaxing some of the relevant bond distances. Actually, the *X*-O2 and *X*-O4 distances are both larger in gadolinite-group minerals with partially or totally occupied *X* sites.

When considering the O5 site, we have the following situations: (1) B at the *Z* site: the O5 coordination is 2 $^{VIII}Ca^{2+}$ + $^{IV}B^{3+}$, yielding 2 × 0.25 + 0.75 = 1.25 v.u. in agreement with the presence of F or (OH); (2) Be at the *Z* site: the O5 coordination is 2 $^{VIII}Y^{3+}$ + $^{IV}Be^{2+}$ + $^{VI}Fe^{2+}$, yielding 2 × 0.375 + 0.50 + 0.333 = 1.583 v.u.; and (3) Li at the *Z* site: the O5 coordination is 2 $^{VIII}Y^{3+}$ + $^{IV}Li^{+}$ + $^{VI}Fe^{3+}$, yielding 2 × 0.375 + 0.25 + 0.50 = 1.50 v.u. Therefore, when Be or Li are incorporated at the *Z* site, the bond-valence incident to O5 is <2. This bond-strength deficiency can be locally compensated by a shortening of the relevant bonds. Actually, gadolinites generally have short *X*-O5 and *A*-O5 distances but long *Z*-O5 distances due to the presence of a larger cation at the *Z* site.

In end-member datolite, where H occupies the *X* site (O5 = OH) there is only one possible arrangement around the O5 site, i.e., 2 $^{VIII}Ca^{2+}$ + $^{IV}B^{3+}$. Accordingly, the FTIR spectrum consists of a single and very sharp band (Fig. 2). In contrast, the spectrum of gadolinite-(Y) from Vico consists of several components (Fig. 2). Figure 5 displays a tentative decomposition of the spectrum of Figure 2, done with the minimum number of Gaussian components, which allows reproduction of the experimental pattern. For gadolinite, the only IR reference is the paper of Ito and Hafner (1974), which reports powder spectra of some natural and synthetic species in the group. Thus, the fitting of Figure 5 is not based on a starting model, and must be considered only as a guide to the eye. Whatever model is used, there are two components with almost equal intensity in the spectrum of gadolinite-(Y) from Vico; they are centered at 3555 and 3520 $cm^{-1}$, respectively. Comparison of the two spectra of Figure 2 suggests the assignment of the band at 3520 $cm^{-1}$ to the local $^{A}$Ca-$^{A}$Ca-$^{Z}$B-$^{O5}$O-H configuration. When we consider the chemistry of the examined sample (Table 1), the band at 3555 $cm^{-1}$ must be assigned to the $^{A}$(REE,Y)-$^{A}$(REE,Y)-$^{Z}$Be-$^{O5}$O-H configuration, because the $^{Z}$B:$^{Z}$Be ratio is close to 1:1, similar to the intensity ratio of the 3555 and 3520 $cm^{-1}$ bands. The band at 3593 $cm^{-1}$ is shifted to higher frequency with respect to the previously discussed bands, hence its assignment must involve a combination of cations yielding an aggregate bond valence on O5 lower than that of the $^{A}$(REE,Y)-

$^{A}$(REE,Y)-$^{Z}$Be configuration. From Table 1, this configuration must involve Li at the *Z* site: $^{A}$(REE,Y)-$^{A}$(REE,Y)-$^{Z}$Li-$^{O5}$OH. The lower-frequency, minor bands at 3482 and 3433 cm$^{-1}$ must be assigned to combination of cations yielding an aggregate bond valence on O5 higher than that of the $^{A}$Ca-$^{A}$Ca-$^{Z}$B configuration. From Table 1, this combination of cations must involve Th+U at the *A* site. In summary, the single-crystal FTIR spectrum of gadolinite-(Y) from Vico is consistent with the presence of several local configurations around the O5 site, and these closely correspond to those predicted on the basis of crystal-chemical considerations.

## Considerations on the existence of "calcybeborosilite"

Both the chemistry (Table 1) and the unit-cell parameters (Table 2) of gadolinite-(Y) from Vico are similar to those reported for "calcybeborosilite-(Y)" (Rastsvetaeva et al. 1996). This evidence raises some doubts on the existence of "calcybeborosilite." In fact, all the details of the chemical and structural analysis reported in this work confirm that the sample from Vico is a Li-rich, Th-rich gadolinite-(Y). The most recent analyses of the material form Dara-i-Pioz (Pekov et al. 2000) show a significant deficit of cations at the *Z* site (around 0.20 apfu). Actually, Pekov et al. (2000) did not analyze Li, which is most likely present also in their sample. In fact, polylithionite and the recently described Li-rich astrophyllite, $Li_2NaFe^{2+}{}_7Ti_2O_2[Si_8O_{24}](OH)_4F$, IMA2006-038, are reported from in the same locality.

Further evidences of the inconsistency of the formula provided by Pekov et al. (2000) can be derived from the structure refinement. In the sample of this work, the refined mean bond-lengths at the tetrahedra (<*T*-O> = 1.629 Å, <*Z*-O> = 1.566 Å) as well as the $^{-O5}$<Z-O> value (1.580 Å) are close to those refined for "calcybeborosilite-(Y)" by Rastsvetaeva et al. (1996), namely 1.629, 1.555, and 1.580 Å, respectively. We can thus conclude that both samples contain almost the same amount of $B_{-1}Be$ substitution at the *Z* site, and do not have major substitution at the *T* site. In contrast, the Be/(B+Be) ratio obtained from the chemical analyses of Pekov et al. (2000) is much lower than in Vico (0.345 vs. 0.574, cf. Table 1), which would correspond to a $^{-O5}$<Z-O> value ~1.525 Å.

The Th and U contents in the sample of Dara-i-Pioz are very low (0.045 apfu). Even if we add the same amount of Li at the *X* site, as suggested by the present work, the *X*-site occupancy is still far lower than 0.5 apfu, and thus this sample should be classified as datolite-(Y), because B > Be. However, Ca is slightly lower than (Y + REE + Th + U), and thus some further analytical problem has to be expected. In particular, spectral interferences in the EMP analyses might have affected the quantification of REE and actinides.

A recalculation of the unit-formula for the sample from Dara-i-Pioz was attempted based on the exchange vectors identified in this work; an hypothetical value of 1.02 $Li_2O$ wt% was used, and all iron was considered in the trivalent state. In this way, we obtained 0.23 $^{Z}$Li apfu and 0.05 $^{X}$Li apfu, balancing for the $^{X}Fe^{3+}$ content (0.23 apfu) and the $^{A}$(Th + U) content (0.05 apfu). The resulting *Z*-site population ($B_{1.15}Be_{0.62}Li_{0.23}$) corresponds to a $^{-O5}$<Z-O> value of 1.576 Å, much closer to the value refined by Rastsvetaeva et al. (1996).

## Concluding remarks

Lithium can be an important constituent of gadolinite-group minerals, and its presence should be systematically checked. Preliminary SIMS data on Alpine gadolinite shows significant quantities of Li at the ppm level [up to 250 ppm in a sample of hingganite-(Y) coming from Cuasso al Monte, Varese, Italy]. Lithium is most likely to occur when (1) the (Th + U) content is significant, or (2) the sum Si + B + Be is lower than 2 apfu. Hence, metamict samples (containing Th and U) should have significant Li contents. This work is part of a more systematic investigation of gadolinites and hingganites; so far, Li was found only at the ppm level in most of the samples examined, but we cannot exclude it might become a major component in suitable geochemical environments.

If the relationship between the $^{X}$Li content and the actinides content is confirmed by further studies on natural and synthetic materials, Li-doped gadolinites could be taken into account for the design of stable forms for radioactive waste disposal.

## Acknowledgments

The authors thank Paola Bonazzi and two anonymous referees for their careful reading of the text and constructive comments. EMP analyses of standard elements were kindly provided by the late Filippo Olmi (CNR-IGG Firenze). This work was supported by funding from CNR to IGG-Unità di Pavia through the project TA01.004.002 and Italian MIUR-PRIN 2005 project "From minerals to materials: crystal chemistry, microstructures, modularity, modulations."

## References cited

Anders, E. and Ebihara, M. (1982) Solar System abundances of the elements. Geochimica et Cosmochimica Acta, 46, 2363–2380.

Anthony, J.W., Bideaux, R.A., Bladh, K.W., and Nichols, M.C. (1995) Handbook of Mineralogy, vol. II, Silicates, 446 p. Mineral Data Publishing, Tucson, Arizona.

Bachechi, F., Federico, M., and Fornaseri, M. (1966) La ludwigite e i minerali che l'accompagnano nelle geodi delle "pozzolane nere" di Corcolle (Tivoli, Colli Albani). Periodico di Mineralogia, 35, 975–1022.

Bellatreccia, F., Cámara, F., and Della Ventura, G. (2006) Datolite: A new occurrence in volcanic ejecta (Pitigliano, Toscana, Italy) and crystal-structure refinement. Rendiconti Lincei Scienze Fisiche e Naturali, 17, 289–298.

Blessing, R.H., Coppens, P., and Becker, P. (1974) Computer analysis of step scanned X-ray data. Journal of Applied Crystallography, 7, 488–492.

Boiocchi, M., Callegari, A., and Ottolini, L. (2006) The crystal structure of piergorite-(Ce), $Ca_8Ce_2(Al_{0.5}Fe^{3+}_{0.5})_{\Sigma1}(\square,Li,Be)_2Si_6B_8O_{36}(OH,F)_2$: A new borosilicate from Vetralla, Italy, with a modified hellandite-type chain. American Mineralogist, 91, 1170–1177.

Burns, P.C., Hawthorne, F.C., Macdonald, D.J., Della Ventura, G., and Parodi, G.C. (1993) The crystal structure of stillwellite. The Canadian Mineralogist, 31, 147–152.

Burragato, F. (1963) Ritrovamento di breislakite in bombe vulcaniche provenienti da una cava di pozzolana nera del Vulcano Laziale. Periodico di Mineralogia, 32, 625–632.

Callegari, A., Caucia, F., Mazzi, F., Oberti, R., Ottolini, L., and Ungaretti, L. (2000) The crystal structure of peprossiite-(Ce), an anhydrous REE and Al mica-like borate with square-pyramidal coordination for Al. American Mineralogist, 85, 586–592.

Della Ventura, G., Parodi, G.C., and Mottana, A. (1990) New rare earth minerals in the sanidinitic ejecta within pyroclastic rocks of the Roman potassic province. Rendiconti Lincei Scienze Fisiche e Naturali, 9, 159–163.

Della Ventura, G., Parodi, G.C., Mottana, A., and Chaussidon, M. (1993) Peprossiite-(Ce), a new mineral from Campagnano (Italy): The first anhydrous rare-earth element borate. European Journal of Mineralogy, 5, 53–58.

Della Ventura, G., Williams, C.T., Cabella, R., Oberti, R., Caprilli, E., and Bellatreccia, F. (1999) Britholite-hellandite intergrowths and associated REE minerals from the alkali-sienitic ejecta of the Vico volcanic complex (Latium, Italy); petrological implications bearing on REE mobility in volcanic systems. European Journal of Mineralogy, 11, 843–854.

Della Ventura, G., Bonazzi, P., Oberti, P., and Ottolini, L. (2002) Ciprianiite and mottanaite-(Ce), two new minerals of the hellandite group from Latium (Italy). American Mineralogist, 87, 739–744.

Demartin, F., Pilati, T., Diella, V., Gentile, P., and Gramaccioli, C.M. (1993) A crystal-chemical investigation of Alpine gadolinite. Canadian Mineralogist,

31, 127–136.
Demartin, F., Minaglia, A., and Gramaccioli, C.M. (2001) Characterization of gadolinite-group minerals using crystallographic data only. The case of hingganite-(Y) from Cuasso al Monte, Italy. Canadian Mineralogist, 39, 1105–1114.
Federico, M. (1957) Sulla breislakite. Periodico di Mineralogia, 26, 191–209.
Foit, F.F., Phillips, M.W., and Gibbs, G.V. (1973) A refinement of the crystal structure of datolite, $CaBSiO_4(OH)$. American Mineralogist, 58, 909–914.
Hawthorne, F.C., Cooper, M.A., Simmons, W.B., Falster, A.U., Laurs, B.M., Armbruster, T., Rossman, G.R., Peretti, A., Günter, D., and Grobéty, B. (2004) Pezzottaite $Cs(Be_2Li)Al_2Si_6O_{18}$ A spectacular new beryl-group mineral from the Sakavalana pegmatite, Fianarantsoa province, Madagascar. Mineralogical Record, 35, 369–378.
Ito, J. (1967) Synthesis of calciogadolinite. American Mineralogist, 52, 1523–1527.
Ito, J. and Hafner, S.S. (1974) Synthesis and study of gadolinites. American Mineralogist, 59, 700–708.
Laurenzi, M.A. and Villa, I.M. (1985) K/Ar chronology of the Vico Volcano (Latium, Italy). IAVCEI, 1985 Scientific Assembly, Giardini Naxos, Italy, Abstract Volume.
Lehmann, M.S. and Larsen, F.K. (1974) A method for location of the peaks in step-scan-measured Bragg reflections. Acta Crystallographica, A30, 580–584.
Locardi, E. (1965) Tipi di ignimbriti di magmi mediterranei. Il vulcano di Vico. Atti Società Toscana di Scienze Naturali, 45, 55–173.
Mandarino, J.A. and Back, M.E. (2004) Fleischer's glossary of mineral species 2004, 309 p. The Mineralogical Record Inc., Tucson, Arizona.
Maras, A., Parodi, G.C., Della Ventura, G., and Ohnenstetter, D. (1995) Vicanite-(Ce): A new Ca-Th-Ree borosilicate from the Vico volcanic district (Latium,Italy). European Journal of Mineralogy, 7, 439–446.
Miyawaki, R., Nakai, I., and Nagashima, K. (1984) A refinement of the crystal structure of gadolinite. American Mineralogist, 69, 948–953.
——— (1985) Structure of homilite, $Ca_{2.00}(Fe_{0.90}Mn_{0.03})B_{2.00}Si_{2.00}O_{9.86}(OH)_{0.14}$. Acta Crystallographica, C41, 13–15.
Nakai, T. (1938) On calciogadolinite, a new variety of gadolinite found in Tadachi, Nagano, Japan. Bulletin of the Chemical Society of Japan, 13, 591–594.
North, A.C.T., Phillips, D.C., and Mathews, F.S. (1968) A semi-empirical method of absorption correction. Acta Crystallographica, A24, 351–359.
Oberti, R., Ottolini, L., Cámara, F., and Della Ventura, G. (1999) Crystal structure of non-metamict Th-rich hellandite-(Ce) from Latium (Italy) and crystal chemistry of the hellandite-group minerals. American Mineralogist, 84, 913–921.
Oberti, R., Della Ventura, G., Ottolini, L., Hawthorne, F.C., and Bonazzi, P. (2002) Re-definition, nomenclature and crystal-chemistry of the hellandite group. American Mineralogist, 87, 745–752.
Ottolini, L. and Oberti, R. (2000) Accurate quantification of H, Li, Be, B, F, Ba, REE, Y, Th, and U in complex matrixes: A combined approach based on SIMS and single-crystal structure refinement. Analytical Chemistry, 72, 3731–3738.
Ottolini, L., Cámara, F., Hawthorne, F.C., and Stirling, J. (2002) SIMS matrix effects in the analysis of light elements in silicate minerals: Comparison with SREF and EMPA data. American Mineralogist, 87, 1477–1485.
Pekov, I.V., Voloshin, A.V., Pushcharovskii, D.Yu., Rastsvetaeva, R.K., Chucanov, N.V., and Belakovskii, D.I. (2000) New data on calcybeborosilite-(Y) $(REE,Ca)_2(B,Be)_2(SiO_4)_2(OH,O)_2$. Vestnik Moscovskogo Universiteta, Geologiya series, 55, 62–70.
Perchiazzi, N., Gualtieri, A.F., Merlino, S., and Kampf, A.R. (2004) The atomic structure of bakerite and its relationship to datolite. American Mineralogist, 89, 767–776.
Rastsvetaeva, R.K., Pushcharovskii, D.Yu., Pekov, I.V., and Voloshin, A.V. (1996) Crystal structure of "calcybeborosilite" and its place in the datolite-gadolinite isomorphous series. Crystallographic Reports, 41, 217–221.
Scherillo, A. (1940) I proietti con minerali boriferi dei vulcani cimini. Periodico di Mineralogia, 11, 367–391.
Segalstad, T.M. and Larsen, A.O. (1978) Gadolinite-(Ce) from Skien, southwestern Oslo region, Norway. American Mineralogist, 63, 188–195.
Shannon, R.D. (1976) Revised effective ionic radii and systematic studies of interatomic distances in halides and chalcogenides. Acta Crystallographica, A32, 751–767.
Sheldrick, G.M. (1997) SHELX-97. Programs for Crystal Structure Determination and Refinement. University of Goettingen, Germany.
Sollevanti, F. (1983) Geologic, volcanologic and tectonic setting of the Vico-Cimino area, Italy. Journal of Volcanology and Geothermal Research, 17, 203–217.
Vaselli, O. and Conticelli, S. (1990) Boron, cesium, and lithium distribution in some alkaline potassic volcanics from central Italy. Mineralogica et Petrographica Acta, 33, 189–204.

MANUSCRIPT RECEIVED JULY 24, 2007
MANUSCRIPT ACCEPTED JANUARY 28, 2008
MANUSCRIPT HANDLED BY PAOLA BONAZZI